sciendo

Research Note • DOI: 10.2478/gsr-2024-0008 GSR • 12 • 2024 • 115–129

Gravitational and Space Research

Formation of three-dimensional (3D) Self-Assembled Clusters of Anisotropic Janus Particles in Microgravity

Jongmin Kim[1], Reya Ganguly[1], Jaesung Kim[1], Ronald J. Sicker[2], Francis P. Chiaramonte[2], William V. Meyer[2], Catherine A. Frey[3], John G. Eustace[3], Deena M. Dombrosky[3], Mark W. Pestak[4], Chang-Soo Lee[1]*

[1]Department of Chemical Engineering and Applied Chemistry, Chungnam National University, 99 Daehakro, Yuseong-gu, Daejeon, 34134 Republic of Korea; [2]USRA at NASA Glenn Research Center, 2001 Aerospace Parkway, MS HX5-2 Brook Park, Cleveland, Ohio, 44152 USA; [3]ZIN Technologies, 6745 Engle Road Airport Executive Park, Cleveland, Ohio, 44130 USA; [4]KBR Wyle Services, Space and Science Business Unit 6749 Engle Road, Cleveland, Ohio 44130 USA

Abstract

The self-assembly of colloidal particles enables the creation of complex materials with tailored properties. This process, particularly involving anisotropic particles, can lead to the formation of structurally unique and complex assemblies that are not achievable with isotropic particles. On Earth, gravitational forces limit the investigation of these particles' intrinsic motion and interactions, posing significant challenges to comprehensively understanding the fundamental forces governing their interactions. To overcome these limitations, this study, in collaboration with NASA's Glenn Research Center (GRC), employs the Light Microscopy Module (LMM) aboard the International Space Station (ISS) to observe the self-assembly phenomena of anisotropic particles under microgravity conditions.

Our investigation shows that anisotropic Janus particles with their distinctive properties can spontaneously organize into ordered structures under microgravity. This directional interaction among anisotropic particles is expected to enable control over assembly processes, forming three-dimensional (3D) clustered structures that are unattainable on Earth. Thus, this study not only advances our understanding of particle self-assembly in microgravity but also opens new avenues for synthesizing materials with novel functionalities through the unique assembly of anisotropic colloids.

Keywords

Anisotropic particles • Microgravity • Self-assembly • Janus particles • directional interaction

Introduction

Colloidal science is an interdisciplinary domain that bridges physics, chemistry, biology, and materials science, exploring the behavior of systems comprising particles dispersed in a continuous medium. These particles, ranging in size from nanometers to micrometers, exhibit unique interactions due to their large surface area-to-volume ratio. The study of colloids encompasses a wide array of materials, including polymers, biological molecules, and minerals, making it fundamental to a broad spectrum of scientific inquiries and technological applications.

Among the phenomena observed in colloidal systems, the concept of self-assembly recently has played a pivotal role in science and engineering. Self-assembly refers to the spontaneous organization of components into structured, functional arrangements, driven by specific, local interactions among the components themselves, without external direction. This process is crucial for constructing complex structures from the bottom up, enabling the creation of materials with novel properties and functionalities.

The significance of self-assembly provides a novel pathway to fabricate materials with precision at the molecular level, allowing for the engineering of micro- and nanostructures with specific optical, electrical, and mechanical properties. These materials have applications in a wide range of fields, from photovoltaics and drug delivery systems to novel catalysts and beyond. Typically, most studies on self-assembly have employed isotropic spherical particles with simple symmetries and isotropic interactions. Due to their isotropic properties, these particles typically self-assemble into packing structures, specifically crystalline structures (Dinsmore et al., 1998; Lin et al., 2000). While isotropic particles serve as excellent building blocks for studying self-assembly and understanding fundamental packing behavior, there is a need to expand the range of chemical and structural (geometrical) complexity of assembled structures for future applications (Glotzer and Solomon, 2007).

Anisotropic particles, characterized by their non-uniform shape or surface chemistry in different directions, contrast with isotropic particles, which have uniform properties regardless of

† Corresponding author: Chang-Soo Lee
E-mail: rhadum@cnu.ac.kr

direction. The anisotropy in particles is granted from various factors, such as elongated shapes (e.g., rods, disks), patches of different chemical compositions on their surfaces, or gradients in material density across the particle. The unique properties of anisotropic particles, compared to isotropic ones, lie in their complex interaction behaviors and the resultant self-assembled structures they can form. Unlike isotropic particles, which may simply aggregate based on the charge or exclude each other due to size, anisotropic particles can align, orient, and assemble into sophisticated, often highly ordered structures due to the directional nature of their interactions. These interactions are governed by the anisotropy in physical forces (like magnetic or electric dipole moments) or chemical affinities (such as hydrophobic or hydrophilic patches) on their surfaces.

However, Earth's gravitational force poses a significant challenge to the study of self-assembly processes, as it influences particle sedimentation and restricts the exploration of intrinsic particle interactions. Specifically, some studies revealed particles and their self-assembled structures are affected by gravitational stress, risking reconfiguration due to sedimentation (Segrè et al., 2001; Senis and Allain, 1997; Weeks et al., 2000). Similarly, other studies reported that the substantial density mismatch in gravity leads to rapid sedimentation and growth kinetics, influencing the equilibrium state of self-assembly (Lee and Furst, 2006; Manley et al., 2004; Sedgwick et al., 2004; Whitmer and Luijten, 2011). Even particles in the tens of nanometers range undergo gravity-induced restructuring, highlighting gravity's profound impact on assembly dynamics (Manley et al., 2004). These limitations underscore the importance of studying colloidal self-assembly under microgravity conditions, where the absence of gravity enables the observation of pure particle interactions and assembly dynamics.

In response to the need for self-assembly studies without the masking effect of gravity, various investigations conducted in microgravity have revealed new scientific phenomena and insights into isotropic particle behaviors. These studies encompass fundamental particle behavior to self-assembled structures including either kinetics of particle growth (Manley et al., 2004) or phase separation (Bailey et al., 2007). Particularly noteworthy was the self-assembly that employed hard spheres in microgravity conducted aboard the Space Shuttle Columbia, which serves as a representative example and sheds light on significant scientific findings regarding the phase differences in assembled crystallization structures between gravity and microgravity conditions (Cheng et al., 2002; Zhu et al., 1997).

Yet, the understanding of particle behavior and the assembly of anisotropic particles in microgravity remains still inadequate. Since the anisotropic particles have greater flexibility in controlling whether there is a geometrical interaction or a chemical interaction, they possess promising potential to introduce more variety in particle motions, interactions by force balance, and directionality, and thereby self-assembly. Comprehensive studies of these anisotropic features without the masking effect of gravity possibly unveil new principles of matter organization, paving the way for the synthesis of materials with unprecedented functionalities.

In this study, we investigate the self-assembly processes of anisotropic particles within the unique confines of a microgravity environment, specifically aboard the International Space Station (ISS), in collaboration with NASA's Glenn Research Center (GRC). Anisotropic particles provide directional interactions that are hypothesized to lead to more complex and ordered structures than those achievable with isotropic particles. To validate this, we design particles with two distinctive anisotropic properties in both chemical and geometrical aspects, referred to as Janus particles, and leverage them as building blocks for self-assembly in the space. Under the microgravity environment of the ISS, we observe fascinating phenomena in particle behavior and interactions, unmasked by the effects of Earth's gravity. This investigation into the mechanisms of directional self-assembly in microgravity contributes significantly to our understanding of colloidal science and materials engineering, potentially paving the way for synthesizing novel colloidal materials.

Materials and Methods

Fabrication of Janus particles with chemical and geometrical anisotropy

Janus particles used in this study exhibit both chemical and geometrical anisotropy. For the chemical aspect, hydrophilicity and hydrophobicity are imparted identically across all three Janus particles. Geometrically, the ratios of hydrophobic to hydrophilic parts are set at 3:7, 5:5, and 7:3, respectively. Additionally, the convex-top geometry is uniformly applied to all three ratios. The Janus particles, with controlled hydrophobic and hydrophilic ratios, were prepared through our sequential micromolding process with slight modifications (Choi et al., 2010; Yeom et al., 2016). Unlike the conventional PDMS mold, a PFPE (Perfluoropolyether dimethacrylate (PFPE-DMA, MD-700), Solvay) mold was prepared and used for reliable particle preparation. First, a photocurable mixture composed of PFPE-DMA and 5% photoinitiator (w/w, darocur 1173 (2-hydroxy-2-methylpropiophenon, Sigma-Aldrich)) was purged by N_2 gas. This mixture was applied to a Si master with predefined SU-8 photoresist patterns (convex-top cylindrical geometry, 3 μm x 5 μm) and photopolymerized into a PFPE mold under ultraviolet (UV) irradiation for 10 minutes in a continuous N_2 gas atmosphere. The hydrophobic photocurable solution, composed of DDDMA (1,10-decanediol

dimethacrylate, polyscience) and 5% (w/w) Irgacure 184 (1-Hydroxycyclohexyl phenyl ketone, Sigma-Aldrich) photoinitiator, was mixed with ethanol at three different volume ratios to prepare anisotropic Janus particles with controlled hydrophobic and hydrophilic ratios (3:7, 5:5, 7:3). The hydrophilic photocurable solution comprised 75% (v/v) PEG-DA (Poly(ethylene glycol) diacrylate, average Mn=700, Sigma-Aldrich), 20% CEA (2-Carboxyethyl acrylate, Sigma-Aldrich), and 5% PETA (pentaerythritol triacrylate, Sigma-Aldrich), with 1% (v/v) darocur 1173 photoinitiator. Each reagent has a distinct function as detailed. PEGDA primarily imparts hydrophilicity to the hydrophilic part of the Janus particles due to its linear ethylene glycol polymeric backbone. CEA further increases hydrophilicity and introduces a slight negative charge due to its carboxylic group, effectively minimizing any non-specific interactions. PETA ensures additional cross-linking density across the hydrophilic part due to three reactive sites, minimizing swelling and maintaining the intended cylindrical geometry. All monomers, along with the initiator, underwent N_2 purging for 1 hour before use. The hydrophobic solution was loaded into the PFPE micromold, the excess solution was removed by pipette suction, and then UV-irradiated in an N_2 atmosphere for 40 seconds to polymerize, creating the hydrophobic part of the Janus particles. Subsequently, the hydrophilic solution was loaded into the mold with the pre-formed hydrophobic part, excess solution removed, and further UV-irradiated in an N_2 atmosphere for 2.5 minutes, completing the formation of the Janus particles. Finally, the collection of the Janus particles from the PFPE mold was achieved through the application of acetone, which serves to gently release the particles without compromising their structural integrity, followed by washing with IPA several times. This methodical approach ensured the precise fabrication of Janus particles with distinct hydrophobic and hydrophilic parts.

Measurement of contact angle for the estimation of free energy of adhesion (ΔG^{ad})

DDDMA hydrophobic and PEG-CEA-PETA hydrophilic films were generated utilizing prepolymer solutions identical to those used for Janus particle preparation. Briefly, each solution was spin-coated onto 3-(Trimethoxysilyl) propyl methacrylate (TPM) pre-coated glass substrates and polymerized under N_2 through UV irradiation. Contact angles were measured using water (W), diiodomethane (DIM), and ethylene glycol (EG) as probe liquids, employing an optical tensiometer (Theta Lite, KSV Instruments, Helsinki, Finland) on each polymeric film.

Loading of Janus particles to the capillary tube and sealing

Before loading the Janus particles into the capillary tube (0.2 mm x 2.0 mm ID, 3520S-050, Vitrocom), PEG silane (2-[Methoxy(Polyethyleneoxy)6-9Propyl] Trimethoxysilane (tech-90, SIM6492.7), Gelest) was coated to prevent nonspecific adhesion of the Janus particles to the tube wall. The capillary was filled with PEG silane using capillary action, followed by thermal incubation at 80°C in a convection oven for 5 minutes. Subsequently, the capillary was thoroughly washed with ethanol and deionized water multiple times, and any residue was removed by N_2 blowing. Next, anisotropic Janus particles with controlled hydrophobic and hydrophilic ratios (3:7, 5:5, 7:3) were initially dispersed in distilled water to a particle volume fraction of 0.004 (v/v, 0.4%), and each dispersion was carefully loaded individually into the PEG-coated capillary tubes to ensure homogeneity. Subsequently, a magnetic stir bar (D x L = 0.1 mm x 1 mm, kindly provided by NASA Glenn) was loaded into the capillary containing the dispersion. To minimize the risk of evaporation, both ends of the capillary tube, containing the particle solution, were securely sealed with the capillary wax (HR4-328, Hampton Research).

Gravity experiment procedure (on Earth)

The capillaries filled with the Janus particles, prepared by the method described in 2.3., were placed on the horizontally balanced optical table, then the characteristics of the Janus particles and their behavior in gravity were observed on an inverted fluorescence microscope (TE2000, Nikon, Japan) equipped with a CCD camera (Coolsnap cf, Photometrics, USA). Image Pro software (Media Cybernetics, Maryland, USA) was used to obtain bright-field microscopy images of the Janus particle geometry, their time-dependent trajectory, and their self-assembled clusters as time increased.

Microgravity experiment procedure (ACE-T-1 mission on ISS)

This study is a part of the series of the colloidal experiment in the ISS, specifically the Advanced Colloids Experiment (ACE) Temperature Control-1 (ACE-T-1). For ACE-T-1 mission on ISS, the Janus particles with three different ratios (3:7, 5:5, 7:3) were loaded into each capillary according to the method described in 2.3., respectively. Then the capillaries were installed in a custom-engineered experimental module designed to establish temperature regulation and magnetic stirring, ensuring controlled experimental conditions. This module was subsequently transported to the ISS using a SpaceX spacecraft and installed in the Light Microscopy Module (LMM) on the ISS, specifically for conducting this space-based experiment. Remote operation of the space microscope from NASA's GRC enabled real-time monitoring of the anisotropic particles' behavior under microgravity. Before the initiation of imaging, a magnetic stir bar within the module was activated at 200 Hz for 1 hour, promoting the thorough mixing and uniform dispersion of the particles within the capillary tube. Imaging commences several

minutes after the cessation of the stir bar's rotation, allowing any flow induced by the magnetic stirring to subside, thus minimizing its influence on the particles' dynamics. Briefly, we used a 2.5x objective to survey the sample and confirm its homogenization. Once homogenization is achieved, images were captured using 10x and 40x magnifications at 9 regions of interest (ROIs), which include the positions of the 5 thermistors and the areas between them. After capturing initial sets of images, a temperature gradient (the maximum gradient is Δ25℃) or a consistent temperature (capable range between 20℃ to 60℃) was determined and applied for one of the predetermined samples to examine the temperature effect on the behavior of particles and their self-assembly. The temperature gradient value or a consistent temperature is controlled as needed throughout the mission. The images captured were transmitted back to NASA's GRC for detailed analysis to elucidate the interactions and assembly behavior of the anisotropic Janus particles under microgravity conditions.

Image analysis

Image J software (http://rsb.info.nih.gov/ij/) was used to characterize the size of the hydrophobic and hydrophilic parts. We measured the dimension of the Janus particles using bright-field microscopic images that were focused on the equatorial (center) plane. In addition, the time-dependent displacement for the estimation of the two-dimensional (2D) translational diffusion coefficient (D_t) of the Janus particles was obtained from the trajectory of the particles analyzed via Image J integrated with PTA and Manual Tracking plugins. The estimated translational diffusion coefficient (D_t) was obtained individually from each data of gravity and microgravity experiment for comparison study.

Results

This study focuses on the anisotropy of the particles, both in their chemical and geometrical aspects, to investigate a potential mechanism for extending the complexity of self-assembled structures. The microgravity environment at the ISS, which is a unique but limited opportunity, permits the observation of distinctive particle behaviors and assemblies, which are phenomena that are obscured by gravitational forces on Earth. Particularly, the objective of the ACE-T-1 experiment is to build a fundamental understanding of the behavior of Janus particles and their interaction under microgravity.

To achieve this, we designed two crucial rules for the Janus particles, one was interparticle interaction and another was the degree of freedom for continuous growth, enabling directionality in their interactions and complexity in self-assembly forms. Firstly, we precisely controlled the directionality of interparticle interaction by utilizing two distinct forces, attraction by hydrophobic interaction and hydrophilic repulsion between Janus particles. To provide these interparticle forces adequately, DDDMA was used for hydrophobic interaction and copolymer of PEG-DA, CEA and PETA were used for hydrophilic repulsion. We postulate that the linear chain of decanediol units in the hydrophobic part of DDDMA, combined with linear ethylene glycol units and the negative charge from carboxyl acid group in the hydrophilic part, establishes a strong hydrophobic interaction on one side and a potent repulsive force on the other side of the Janus particle. This dual nature as chemical anisotropy on opposite sides of the Janus particle enables a precisely controlled interparticle interaction.

Estimation of hydrophobic interaction and hydrophilic repulsion

To validate this, the hydrophobic interaction and hydrophilic repulsion between particles are approximately estimated by the theoretical thermodynamic free energy of adhesion (ΔG^{ad}). Briefly, the surface free energy of each hydrophobic and hydrophilic part is first calculated by using contact angles' values of three different liquids, (Water (W), diiodomethane (DIM), and ethylene glycol (EG)), measured on each hydrophobic and hydrophilic film, and the van Oss-Chaudhury-Good (vOCG) equation (1) and equations (2, 3) (Vanoss et al., 1988).

$$\gamma_L(1+cos\theta) = 2\sqrt{\gamma_s^{LW}\gamma_L^{LW}} + 2\sqrt{\gamma_s^{+}\gamma_L^{-}} + 2\sqrt{\gamma_s^{-}\gamma_L^{+}} \quad (1)$$

$$\gamma_s^{AB} = 2\sqrt{\gamma_s^{+}\gamma_L^{-}} \quad (2)$$

$$\gamma_s^{total} = \gamma_s^{LW} + \gamma_s^{AB} \quad (3)$$

Then, the interfacial free energies per unit contact area solid–liquid (γ_{13}, γ_{23}) and solid–solid (γ_{12}) interactions are determined using the surface free energy values (γ^{tot}, γ^{LW}, γ^{+}, γ^{-}) of the hydrophobic part, hydrophilic part, polar solvent, and equation (4) (Vanoss et al., 1988).

$$\gamma_{ij} = \gamma_i + \gamma_j - 2\sqrt{\gamma_i^{LW}\gamma_j^{LW}} - 2\sqrt{\gamma_i^{+}\gamma_j^{-}} - 2\sqrt{\gamma_i^{-}\gamma_j^{+}} \quad (4)$$

Finally, we examined the free energy of adhesion (ΔG^{ad}) per unit contact area between the Janus particles (e.g., hydrophobic (γ_1) and hydrophilic (γ_2) parts) immersed in the assembly media (γ_3) by using the evaluated each interfacial free energy and equation (5, 6).

Table 1. Theoretically estimated surface free energy of the Janus particles and their free energy of adhesion in water.

Polymeric surfaces	Contact angle [°]			Surface free energy components [mJ/m²]			
	Water	DIM	EG	γ_s	γ_s^{LW}	γ_s^+	γ_s^-
DDDMA (hydrophobic part)	108.33	46.60	56.42	36.15	36.15	1.11	[a]0
PEGDA-CEA-PETA (hydrophilic part)	35.95	41.25	45.44	38.98	38.98	[a]0	60.73
Water	-	-	-	[b]72.8	[b]21.8	[b]25.5	[b]25.5
Janus particles (Hydrophobic/Hydrophilic)	Thermodynamic free energy of adhesion (ΔG^{ad}) [mJ/m²]						
	Hydrophilic-Hydrophilic part			Hydrophobic-Hydrophobic part			
DDDMA/PEGDA-CEA-PETA	50.46			-84.37			

[a]Negative value was considered to be zero (Tadros, 2015).
[b]Values were reported in the literature (Grzybowski et al., 2003).

$$\Delta G_{131}^{ad} = -2\gamma_{13} \quad (5)$$

$$\Delta G_{232}^{ad} = -2\gamma_{23} \quad (6)$$

The measured contact angle and estimated free energy of adhesion is shown in **Table 1**. The distinct contact angles of water (CA=108.33°±2.22°) on the DDDMA polymeric films, clearly demonstrate it is hydrophobic, whereas the contact angle of an air bubble on the PEG-CEA-PETA film immersed in water (CA=35.95°±0.46°) is much lower, meaning it is hydrophilic. Evaluating the surface free energy components reveals that the apolar component (γ_s^{LW}) of the DDDMA surface is 36.15 mJ/m², while the Lewis acid and base components are negligibly small. This emphasizes the hydrophobic nature of the DDDMA part in the Janus particles, in line with the water contact angle results. Conversely, the PEG-CEA-PETA surface exhibits a surface free energy of 60.73 mJ/m² for the Lewis base component (γ_s^-), with the Lewis acid component (γ_s^+) being negligibly small, indicating the hydrophilicity and monopolarity of the PEG-CEA-PETA part in the Janus particles. The calculated free energy of adhesion (ΔG^{ad}) between hydrophobic DDDMA surfaces yields a highly negative value (-84.37), indicating a potential for spontaneous attraction through hydrophobic interaction. In contrast, the free energy of adhesion between hydrophilic PEG-CEA-PETA surfaces is significantly positive at +50.46, clearly indicating non-attraction, as detailed in **Table 1**. This non-attraction is likely attributed to the monopolar properties of the PEG-CEA-PETA surface, showcasing the ability to repel each other in polar solvents such as alcohol and water (Napper, 1983; Oss, 2006).

These results strongly support the anticipated precisely controlled interparticle interaction and their directed assembly of Janus particles through the combination of hydrophobic interaction and hydrophilic repulsion.

Next, the second design rule involved granting a degree of freedom for the continuous growth of self-assembled structures by finely tuning the geometry of the Janus particles. Beyond simple structures or small clusters such as dimers (N=2), constituted by interaction of a few Janus particles, we hypothesized that this continuous growth demands securing sufficient hydrophobic parts remaining even after the initiation of self-assembly. Furthermore, hydrophilic body should possess a minimal area to easily allow additional joining of the Janus particles to the initially formed assembled structures. For this, we designed the hydrophobic part of the Janus particles using convex-top geometry with a cylindrical body, which likely forms the self-assembled structure through minimal area interaction of the hydrophobic area and enabling its continuous growth without steric hindrance. To further enhance the degree of freedom for continuous growth, we hypothesized that convex-top Janus particles in the aqueous solution, varying in their ratios of hydrophilic to hydrophobic parts, are used for the experiment of self-assembly, and can form three distinct types of pairwise assemblies by hydrophobic interaction: tip-to-tip, tip to side, and side-to-side. Here, 'tip' refers to the small contact area of hydrophobic part, and 'side' refers to the lateral aspect of the hydrophobic part of the Janus particle, respectively.

Taken together, the two design rules for both interparticle force controlled via hydrophobic interaction and hydrophilic repulsion, and the degree of freedom for continuous growth affected by controlling hydrophobic and hydrophilic ratio with convex-top on the cylindrical body of the particles, we expected the behavior of the Janus particles and their self-assembly (**FIG. 1**). First, the thermodynamic principles guide particle interaction, with red representing hydrophobic parts and blue representing hydrophilic parts. A thermodynamically favorable configuration is achieved when the hydrophobic parts interact (ΔG_{131}^{ad}<0), whereas a repulsive force predominates between hydrophilic parts (ΔG_{232}^{ad}>0) (**FIG. 1A**). Once the initial assembled structure is formed, the

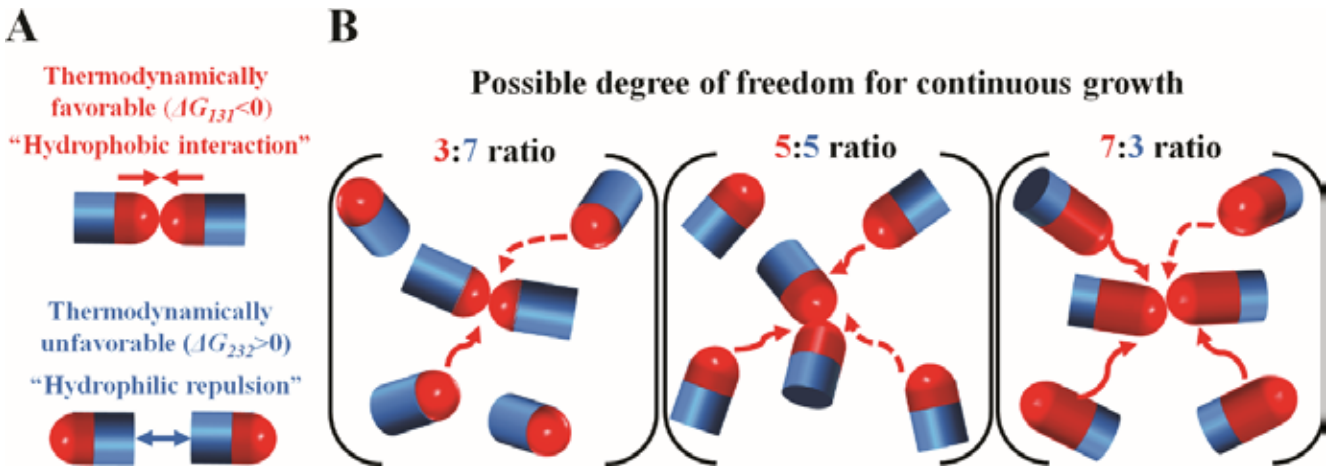

Figure 1. Two crucial design principles for Janus particles based on chemical and geometrical anisotropy, and expectation on possible degree of freedom for continuous growth controlled by the ratio between hydrophobic and hydrophilic parts of the Janus particles. (A) Chemical anisotropy of the Janus particle: Precise control of interparticle interaction involving hydrophobic interaction and hydrophilic repulsion. (B) Geometrical anisotropy of the Janus particle: The hydrophobic (red) and hydrophilic (blue) ratio of the Janus particles possibly affects the interaction between initially assembled structures and free Janus particles, allowing different degrees of freedom for continuous growth during the self-assembly. For example, a 3:7 ratio allows interaction with 1 or 2 more Janus particles, 5:5 with 2 or 3 more, and 7:3 with 3 or 4 more. The additional geometrical anisotropy in the form of a convex-top design plays a role by enabling hydrophobic interactions with minimal contact area, thereby supporting continuous growth.

ratio of hydrophobic and hydrophilic parts has significant potential to consecutively influence the degree of freedom for continuous growth. Presumably, the ratio of 3:7 may afford additional interaction with 1 (solid) or 2 (dash) free Janus particles, while the ratio of 5:5 may provide the freedom for interaction with 2 (solid) or 3 (dash) more Janus particles, and the ratio of 7:3 could allow interaction with 3 (solid) or 4 (dash) more Janus particles. Solid and dashed arrows represent higher or lower probabilities of interaction, respectively. This determination is based on the ratio between the hydrophobic and hydrophilic parts, the kinetic behavior of particles, and their thermodynamic equilibrium (**FIG. 1B**).

Fabrication and characterization of Janus particles

In alignment with the two critical design rules, the Janus particles, featuring a convex-top and a cylindrical body with precisely controlled hydrophilic and hydrophobic ratios, are produced through sequential micromolding. (Choi et al., 2010; Yeom et al., 2016). Briefly, a hydrophobic photocurable solution based on DDDMA is loaded into a PFPE micromold, then evaporation of diluent and subsequent irradiation of UV resulted in polymerization of formation of the hydrophobic part with a different ratio for the amount of the mixed diluent. Subsequently, a hydrophilic photocurable solution composed of PEG-DA, CEA, and PETA is loaded and polymerized via UV exposure, resulting in a convex-top Janus particle. The bright-field image shows reliable fabrication of the convex-top Janus particles with three different ratios via micromolding. The convex-top Janus particles are highly uniform in both geometry and size which is aligning precisely with the predesigned pattern of the PFPE micromold (**FIG. 2A**). The relatively different contrast in a Janus particle shown in the enlarged inset image of the **FIG 2A** is showing the boundary of two different parts: the hydrophobic part (dark) and hydrophilic part (bright) as designed. The controlled ratio between the hydrophobic and hydrophilic parts is a key geometrical anisotropy in our Janus particles, which plays a pivotal role in the ratio-dependent self-assembly, as elaborated-on in **FIG. 1.** Hence, precise characterization of this controlled ratio in the Janus particle is a critical prerequisite before proceeding with the valuable space experiments.

Quantitative analysis clearly demonstrates the high uniformity in ratios, aligning closely with the targeted proportions of 3:7, 5:5, and 7:3 (**FIG. 2B**). These results clearly indicate that micromolding enables reliable preparation of the convex-top Janus particle with the sizes as well as the controlled geometry as designed.

Self-assembly of Janus particles in gravity (on Earth)

Preceding the space experiments, behavior of the convex-top Janus particles with varying ratios (3:7, 3:3, 7:3) and their self-assembly in aqueous solution are investigated under the Earth's gravitational forces for a comprehensive understanding of self-assembled structures and Brownian motion (**FIG. 3**). The Janus particles, characterized by their distinct hydrophobic and hydrophilic parts as chemical anisotropy, demonstrate directional interaction due to their inherent interaction forces between hydrophobic parts and the

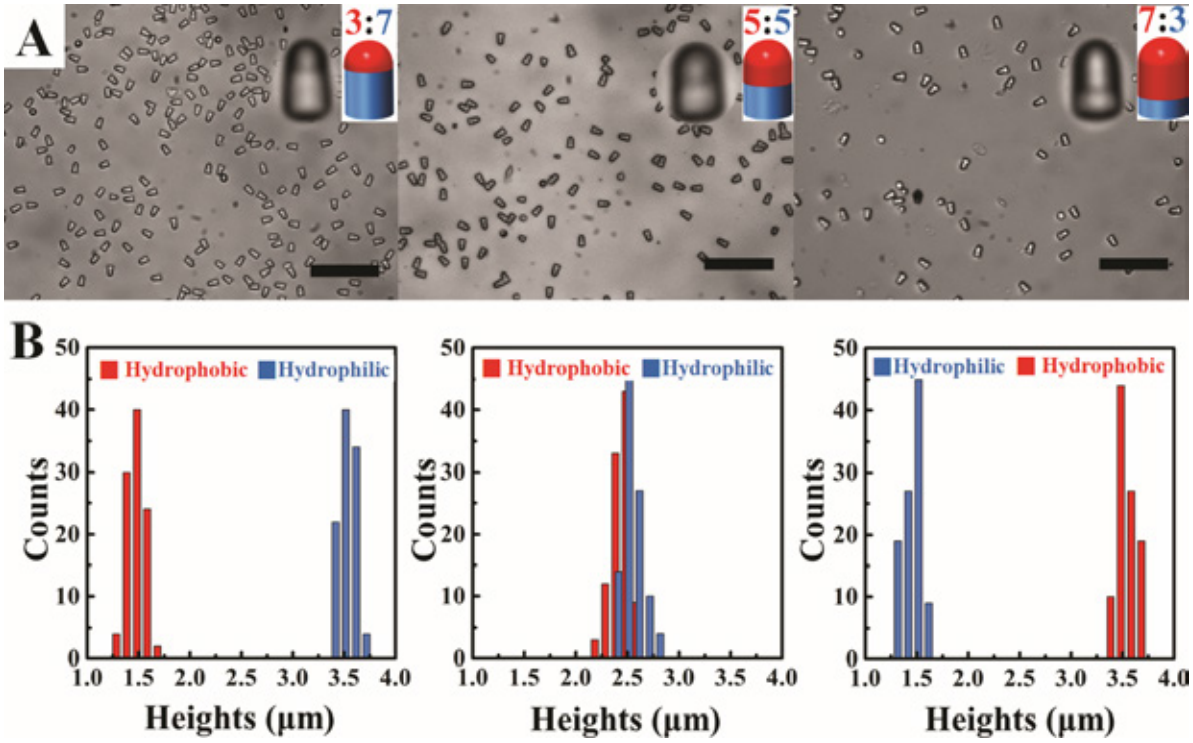

Figure 2. Convex-top Janus particles with three different ratios (3:7, 5:5, 7:3) of hydrophobic and hydrophilic parts showing the geometrical anisotropy. (A) Schematic images and brightfield images showing uniformly controlled geometric aspects: the three different ratios (3:7, 5:5, 7:3) and the convex-top. In the inset images of the Janus particles, the hydrophobic parts are notably darker, while the hydrophilic parts appear brighter, highlighting the clear boundary between these distinct parts. (B) Quantitative analysis illustrating the geometrical anisotropy, ratios of the hydrophobic and hydrophilic parts of the convex-top Janus particles as designed (3:7, 5:5 and 7:3). Scale bars in all images are 30 μm.

repulsive force between hydrophilic parts. **FIG. 3A** shows the representative self-assembled clusters and their type of pair configurations formed via self-assembly for each of the Janus particles (3:7, 5:5, 7:3).

The optical images show the formation of the dimer (N=2) on a 2D planar plane through hydrophobic interactions between the convex-top Janus particles, suggesting that the reduction in surface-free energy is the predominant driving force behind the interactions in this particular geometric arrangement. Unexpectedly, the predominant configurations consist mainly of 2D dimers on a planar plane, regardless of the hydrophobic to hydrophilic ratio in the Janus particles. This observation might be a result of the limited time available for the Janus particles to undergo additional interparticle interactions, influenced by gravitational forces. In contrast, the ratio between the hydrophobic and hydrophilic parts of the Janus particles likely affects the pair configuration of the assembled clusters. The 3:7 Janus particles predominantly assemble in the tip-to-tip configuration (67%), with the remainder formed by the tip-to-side (33%) configuration. Interestingly, the 5:5 ratio exclusively shows the tip-to-side configuration (100%), while the 7:3 ratio exhibits the prevailing tip-to-side configuration (83%) with a minor fraction in the side-side configuration (17%). The different favorable configurations of the three different ratios (3:7, 5:5, 7:3) are presumably determined by a force balance between the hydrophobic interaction and hydrophilic repulsion of the Janus particle. As the particles approach to interact with each other, two forces act simultaneously: hydrophobic interactions minimize the unfavorable interface between the hydrophobic parts and water, whereas hydrophilic repulsion facilitates the formation of a favorable interface between the hydrophilic parts and water, along with repulsion between the particles. At this stage, the Janus particle configuration is governed by the ratio of their hydrophobic and hydrophilic parts. In the 3:7 ratio with a larger hydrophilic part, hydrophilic repulsion becomes dominant while hydrophobic interactions play a minimal role in particle orientation. The larger repulsive hydrophilic part favors aligning the hydrophilic parts of the particle spatiotemporally farthest away from each other to form a larger interface with water, allowing for the majority of the tip-to-tip configuration. In contrast, in the 7:3 ratio with a larger hydrophobic part, hydrophobic interactions become dominant while hydrophilic repulsion plays a minimal role in particle orientation. Considering the entire interface between

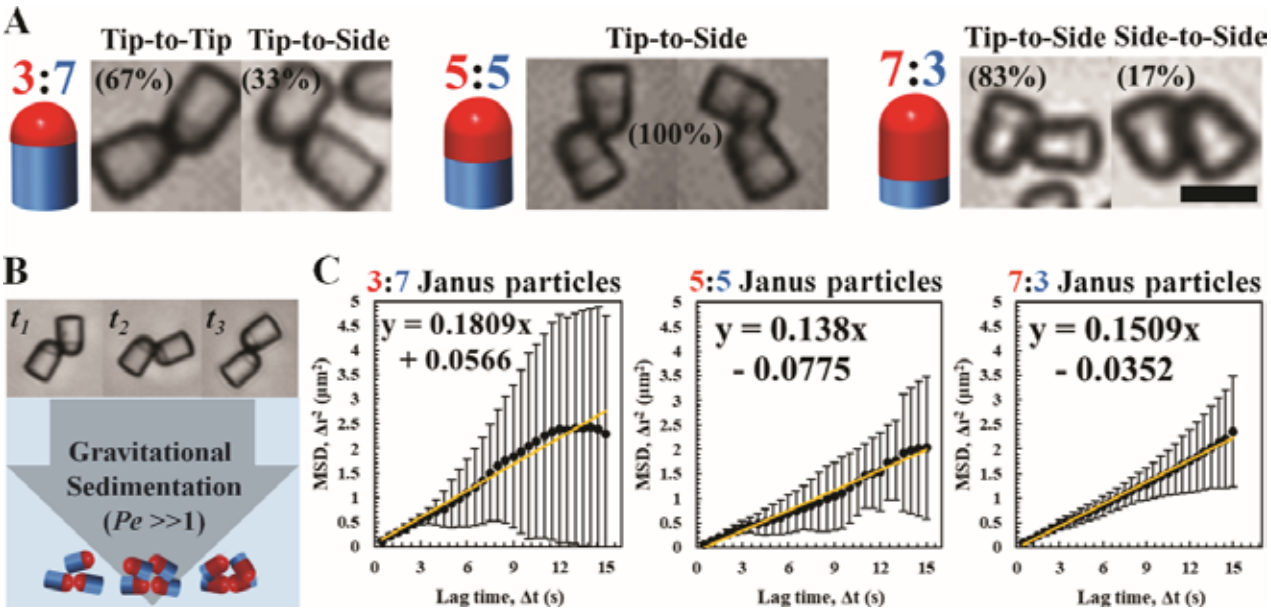

Figure 3. 2D assembly of convex-top Janus particles under gravity. (A) The representative self-assembled 2D clusters and their type of pair configurations formed via self-assembly of each Janus particles (3:7, 5:5, 7:3). (B) Sequential time-lapse images showing the formation of the limited small dimer (N=2) staying at a similar position with a slight orientation change over time. This result demonstrates gravitational sedimentation severely interferes with the movement of particles as well as their self-assembly. (C) 2D mean squared displacement (MSD) of each of the convex-top Janus particles (3:7, 5:5, 7:3) in gravity. A slope (yellow) of the solid line divided by 4 yields the 2D translational diffusion coefficient of each convex-top Janus particle. Scale bars in the image showing the 7:3 Janus particle is 5 μm.

Janus particles with water, a larger thermodynamically unfavorable interface is formed at the 7:3 ratio than at the 3:7 ratio, which needs to be minimized promptly. At this stage, the two configurations: tip-to-side and side-to-side, which minimize the larger interface with water, become dominant over tip-to-tip. However, the hydrophilic repulsion is not strong enough for reorientation, so the majority remains in the tip-to-side configuration, which is assumed to be the initial contact during particle interaction. In the case of a 5:5 ratio, the size of each part is identical, allowing a balanced contribution of hydrophobic interaction and hydrophilic repulsion to particle orientation. Hydrophobic interactions aim to reduce free energy by minimizing hydrophobic interfaces with water, while hydrophilic repulsion favors the formation of hydrophilic interfaces with water, but is not strong enough to keep the particles farthest away from each other. This balanced contribution of the two forces results in the exclusive formation of the tip-to-side configuration.

These configuration differences even in gravity provide promising expectations that the degree of freedom can potentially be altered depending on the ratio of the hydrophobic and hydrophilic parts of the Janus particles. The analysis of time-lapse images (t_1, t_2, t_3) shows the progressive stages of particle interaction (**FIG. 3B**). However, a significant number of the Janus particles sediment before larger cluster formation, primarily as a consequence of gravitational forces.

We further estimate the gravitational Péclet number (*Pe*), which is a dimensionless quantity describing the ratio of the time of the Brownian diffusion (τ_B) against that of sedimentation (τs) of particles, using the equation (7) (Lee and Furst, 2006; Whitmer and Luijten, 2011).

$$Pe = \frac{\tau_B}{\tau_s} = \frac{\sigma}{2l_g} = \frac{\pi\sigma^4\Delta\rho g}{12k_BT} \quad (7)$$

Where σ is the diameter of the particle, l_g is the gravitational length, $\Delta\rho = |\rho_p - \rho_s|$ is the density difference between the particle and the solvent, g is the gravitational acceleration, and k_BT is the thermal energy. The calculated *Pe* on Earth is 77.083 (*Pe* >> 1), indicating that gravity significantly influences the particles, with sedimentation prevailing over Brownian motion. In practical terms, this means that particles descend so rapidly due to gravity that there is inadequate time and velocities for them to fully explore the phase space of positions essential for thermodynamic assembly processes.

In addition, it's important to note that the gravitational *Pe* reflects the characteristics of individual particles, meaning the impact of gravity can be substantially different at assembled clusters. For instance, once the Janus particles form self-assembled clusters, the relevant buoyant force is not that of the single Janus particle but rather the force experienced

by assembled clusters consisting of multiple numbers of the Janus particles.

Subsequently, evaluating the translational diffusion coefficient of convex-top Janus particles in a gravitational field and conducting a comparative study against the theoretically estimated diffusion coefficient is meaningful for a more in-depth understanding of particle behavior. To achieve it, 2D locational displacement (x, y) of a single particle is obtained by tracking the single particle, and all displacements in both the x- (e.g. $\Delta x_1=x_1- x_0$) and y-direction (e.g. $\Delta y_1=y_1-y_0$) derived from the 2D trajectory as a function of time are obtained. Next, squared total displacement (Δr^2) is calculated by the squaring and summation of each displacement ($\Delta r^2=\Delta x^2+\Delta y^2$). Then, MSD ($\langle\langle(\Delta r^2)\rangle\rangle$) is computed by averaging Δr^2, which is obtained from 10 particles' tracking analysis.

In **FIG. 3C**, the MSD over time of each convex-top Janus particle (3:7, 5:5, 7:3) is shown. In 2D, the time-dependent MSD can be expressed as $\langle(\Delta r^2)\rangle=4D_t\cdot\Delta t$. By dividing the slope obtained from linear regression by 4, the translational diffusion coefficients (D_t) for each convex-top Janus particle are derived. The estimated diffusion coefficient describes the behavior of particles diffusing through a medium, which has a high correlation with the movement and interaction of particles and collision frequency, thereby understanding self-assembly. The calculated translational diffusion coefficients (D_t) for the convex-top Janus particles are 4.523×10^{-2} μm²/s (3:7 ratio), 3.450×10^{-2} μm²/s (5:5 ratio), and 3.773×10^{-2} μm²/s (7:3 ratio), respectively. Unfortunately, there is no significant correlation between the ratio of the Janus particles and the diffusion coefficient, which may be hindered due to gravity. For comparison, the theoretical diffusion coefficient is computed using the bead shell-based cylinder model equation (8) (Carrasco and de la Torre, 1999; Delatorre and Bloomfield, 1981; Ortega and de la Torre, 2003; Tirado et al., 1984). Here, η represents the fluid viscosity, while L and d denote the length and diameter, respectively, and C_t stands for a numerical constant.

$$(D_t = \frac{k_B T}{3\pi\eta L}(ln(L/d) + C_t)) \quad (8)$$

The convex-top Janus particle exhibits exceptional chemical and geometrical anisotropy, so pinpointing an ideal theoretical model for Janus particles proves challenging. To the best of our knowledge, the bead shell-based cylinder model provides a valuable initial framework for comprehending particle behavior. The theoretically computed diffusion coefficient as 9.658×10^{-2} μm²/s reveals that the Brownian diffusion of the Janus particle in gravity is approximately 2 or 3 times less than the theoretical model. Therefore, the constrained motion of Janus particles, caused by gravitational stress, is believed to restrict additional freedom in interparticle interaction, consequently hampering the formation of larger or more intricate clusters.

Self-assembly of Janus particles in microgravity (on ISS)

Next, we perform the ACE-T-1 space experiment to investigate promising design parameters for enabling selective interactions with directional specificity to build complex structures of significance. Utilizing the LMM at ISS, our research investigates the controllability of Janus particles to pioneer the construction of three-dimensional (3D) structures. The optical images in **FIG. 4** reveal the distribution of 3D clusters formed by convex-top Janus particles through hydrophobic interactions and hydrophilic repulsions under microgravitational conditions. As designed, the chemical anisotropy comprises hydrophobicity and hydrophilicity to effectively enable directional interaction of the Janus particles. These 3D clusters originate from a combination of three configurations, tip-to-tip, tip-to-side, and side-to-side, within the hydrophobic parts of particles characterized by the convex-top geometry. Unlike the bidirectional interactions on the planar plane of Earth that result in 2D assemblies, the clustering of convex-top Janus particles exhibits multiaxial orientations in 3D space. This complexity renders it statistically challenging to classify these assemblies into a specific configuration. (**FIG. 4A**). Observation of these 3D clusters, which consist of the same number of particles but exhibit distinct spatial orientations, allows us to deduce that upon initial contact, two Janus particles can readily reorient to establish energetically more favorable assemblies. This adaptability in altering their interparticle configurations sharply contrasts with the behavior of chemically homogeneous cylinders, which tend to form robust capillary bridges between their planar end surfaces, resulting in the formation of linear chains. This distinct difference is attributed to the unique interactive dynamics of Janus particles compared to their chemically uniform counterparts, implying their potential for creating complex, energy-efficient structures.

FIG. 4B demonstrates representative forms of assembled 3D clusters under microgravity using each of the Janus particles. Unlike the results on Earth, it is observed that the cluster size and form are significantly influenced by the hydrophobic part. Typically, the Janus particles with small hydrophobic parts self-assemble into seed clusters containing mainly dimers (N=2) and trimers (N=3) or a few of multimers (N≥4) in spherical-like form. In contrast, particles with large hydrophobic parts self-assemble into densely packed or linearly grown forms composed mainly of more multiparticles (N≥4). This result can likely be attributed to the combined effects of geometry and chemical properties.

Through localized contact attributed to the convex-top geometry, primarily in a tip-to-tip configuration, small seed

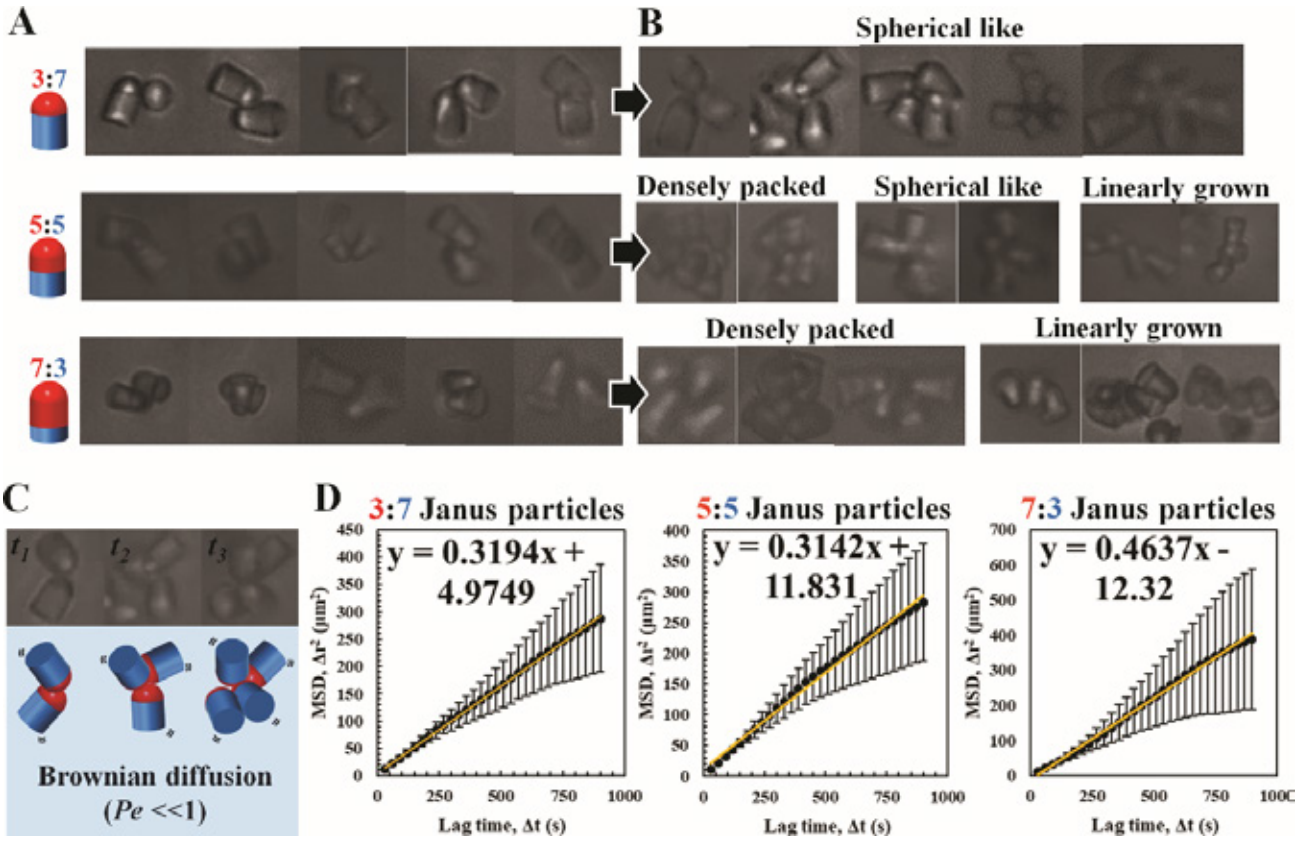

Figure 4. 3D assembly of convex-top Janus particles in microgravity. (A) The representative self-assembled 3D dimers (N=2) and their various multiaxial orientation pair configurations formed via self-assembly of each of the Janus particles (3:7, 5:5, 7:3). (B) Various forms of self-assembled 3D clusters such as spherical-like, densely packed, and linearly grown clusters that are thermodynamically favorable and considered an equilibrium state. (C) Sequential time-lapse images showing an initially assembled dimer (N=2) of the convex-top Janus particle and its continuous growth over time to tetramer (N=4). (D) 2D MSD of each convex-top Janus particle (3:7, 5:5, 7:3) in microgravity. A slope (yellow) of the solid line divided by 4 yields a 2D translational diffusion coefficient (D_t) of each convex-top Janus particle.

clusters are initially formed. In this state, there are still many remaining hydrophobic areas in the pre-formed small clusters that can potentially interact with other individual Janus particles, which is a favorable environment for continuous cluster growth. Then, the equilibrium states exhibited by the final assembled clusters are mainly determined by the ratios of hydrophobic and hydrophilic parts. In particular, the 7:3 Janus particle, characterized by the largest hydrophobic part, demonstrates the highest degree of freedom for continuous growth. This is attributed to the substantial residual hydrophobic part on the initial seed cluster, enabling interactions with subsequently joining particles from any axial orientations. As a result, this promotes the formation of clusters with linear growth or dense packing. In the case of the 3:7 ratio, which is characterized by the smallest hydrophobic part, the predominant form of the self-assembled structure consists of loosely arranged, 3D spherical-like clusters. Although the initial seed cluster formed by 3:7 Janus particles possess a relatively smaller degree of freedom for continuous growth due to the smallest hydrophobic part, there is still remaining space on the hydrophobic part, making it thermodynamically favorable for continuous growth. However, as the growth proceeds, the remaining hydrophobic space diminishes, necessitating specifically oriented access for the next joining particles. Moreover, relatively stronger hydrophilic repulsion from the largest hydrophilic part coexists which supports the center orientation of particles more precisely. This leads to the enforcement of center-oriented hydrophobic parts in self-assembled clusters, resulting in loosely arranged 3D spherical-like clusters. The 5:5 Janus particle, with an intermediate proportion of hydrophobic parts between 3:7 and 7:3, exhibits characteristics of both, thereby forming all types of structures including linearly grown or loosely arranged spherical-like or densely packed clusters. In other words, the results described in **FIG. 4B** indicate that the final structure of the assembled clusters can be designed by manipulating the geometrical aspect, specifically the ratios of hydrophobic and hydrophilic parts of the Janus particles.

The optical images obtained under microgravity align with the 3D illustrations in **FIG. 4C**, depicting the temporal evolution and spatial arrangement of 3:7 convex-top Janus particle assembly. In the unique microgravity environment devoid of gravitational sedimentation (estimated Pe=7.78×10^{-5}), the Janus particles are actively and freely exploring the full phase space of positions, allowing the formation of the 3D cluster. Once aligned with thermodynamically favorable orientations, they likely maintain their initial configuration stability until interacting with other particles. These unique assembly systems allow for the stable formation of seed clusters (N=2) with spatially diverse orientations that maintain a high degree of freedom for continued growth, resulting in a variety of 3D clusters ranging from those that are spherical-like, densely packed, to linearly grown forms.

Moreover, the unique environment provided by microgravity uncovers the hidden fundamental kinetic information of the Janus particles. It is important to note that the fascinating microgravity conditions allow the Janus particles to actively explore 3D spaces, which is highly promising. However, we encounter challenges in analyzing their 3D trajectories. The particle selected for tracking frequently and completely moves out of the microscope's focal plane, which leads to analytical challenges in obtaining Z-axis displacement once the particle disappears. Consequently, conducting our tracking and analysis solely in 2D trajectories is inevitable.

FIG. 4D shows translational diffusion coefficients (D_t) of each of the Janus particles (3:7, 5:5, 7:3) under microgravity, as evaluated by analyzing 2D trajectory. Compared to the diffusion coefficient obtained in gravity, we confirm that each diffusion coefficient of the particles for 3:7 (8.618×10^{-2} μm²/s), 5:5 (9.785×10^{-2} μm²/s), and 7:3 (9.378×10^{-2} μm²/s) closely match the theoretically estimated diffusion coefficient (D_t=9.658×10^{-2} μm²/s) for a bead shell-based cylinder. Unfortunately, the effect and correlation of the ratio of hydrophobic and hydrophilic parts on the diffusion coefficient remained unclear. This may be due to several differences between the Janus particles and the theoretical model. For example, the theoretical model is based on a cylinder with flat-ends at both sides, but the Janus particle is a cylinder with a convex-top and a flat-end. In addition, the theoretical value is considered for the aspect ratio (AR)>2, which is quite larger than the AR of the sample (AR≈1.67). Furthermore, the Janus particles are chemically anisotropic and composed of both hydrophilicity and hydrophobicity.

Overall, this experimental result strongly suggests that the absence of gravity permits a more accurate characterization of the particles' behavior, unaffected by the sedimentation that occurs on Earth. This could potentially lead to the discovery of new self-assembling structures and mechanisms, contributing to the advancement of material science and engineering.

Next, ACE-T-1 mission's notable advancement over previous NASA colloidal science missions is the ability to control the temperature of sample cells. This capability allows for an in-depth exploration of Janus particles' behavior in microgravity under precisely controlled temperatures, encompassing particle kinetics, thermal interactions, and self-assembly. For this purpose, we conduct a detailed analysis of cluster formation among Janus particles with a hydrophobic-to-hydrophilic ratio of 7:3 and quantitatively evaluate the motion of the Janus particles at different temperatures. ACE-T-1 utilizes capillary cells, and one set of three capillary cells is provided for each sampling module. On a stage with temperature control, three capillary cells can be positioned so that a uniform temperature can be set for the entire sample, or a temperature gradient can be placed along the length of the capillaries (typical range: 20–60°C, 10°C temperature differential over the length of the capillary) or between the bottom and top of a capillary in case an oil immersion objective is used as a cold sink (which remains close to ambient temperature, around 20°C).

FIG. 5 presents a pivotal discovery from the ISS experiments regarding the temperature-dependent dynamics of anisotropic Janus particle assemblies. **FIG. 5A** shows the MSD analyzed over increasing lag times (Δt) for 7:3 Janus particles, providing quantitative insights into particle mobility at 20°C and 60°C. At 60°C, the particles exhibit significantly higher MSD, indicating enhanced kinetics of the particles, compared to their behavior at 20°C. Interestingly, the inset images in **FIG. 5A** reveal that the 3D structures formed by self-assembly at each temperature differ markedly: complex 3D clusters with smaller contact areas form at 60°C, while less complex 3D clusters with larger contact areas form at 20°C.

FIG. 5B suggests that the variation in 3D assemblies at different temperatures is presumably due to variations in particle dynamics and interparticle forces. The formation of complex 3D clusters with smaller contact areas at 60°C is likely attributed to increased particle kinetics and hydrophobic interactions. Elevated temperatures enhance particle kinetics, increasing interaction opportunities between particles and pre-assembled seed clusters. In the case of hydrophobic interaction, it is known to increase as temperature increases (Baldwin, 1986; Claesson et al., 1986; Kegel and van der Schoot, 2004) because of its endothermic nature (Némethy and Scheraga, 1962). Therefore, we hypothesize that elevated temperature imparts strong enough hydrophobic interaction to form self-assembly with a smaller contact area between hydrophobic parts. This cluster still provides many leftover areas for continuous growth, allowing additional interaction with kinetically increased particles. However, at a relatively lower temperature at 20°C, relatively less kinetics of particles and weaker hydrophobic interactions necessitate larger contact areas for equilibrium, resulting in less complex 3D assemblies.

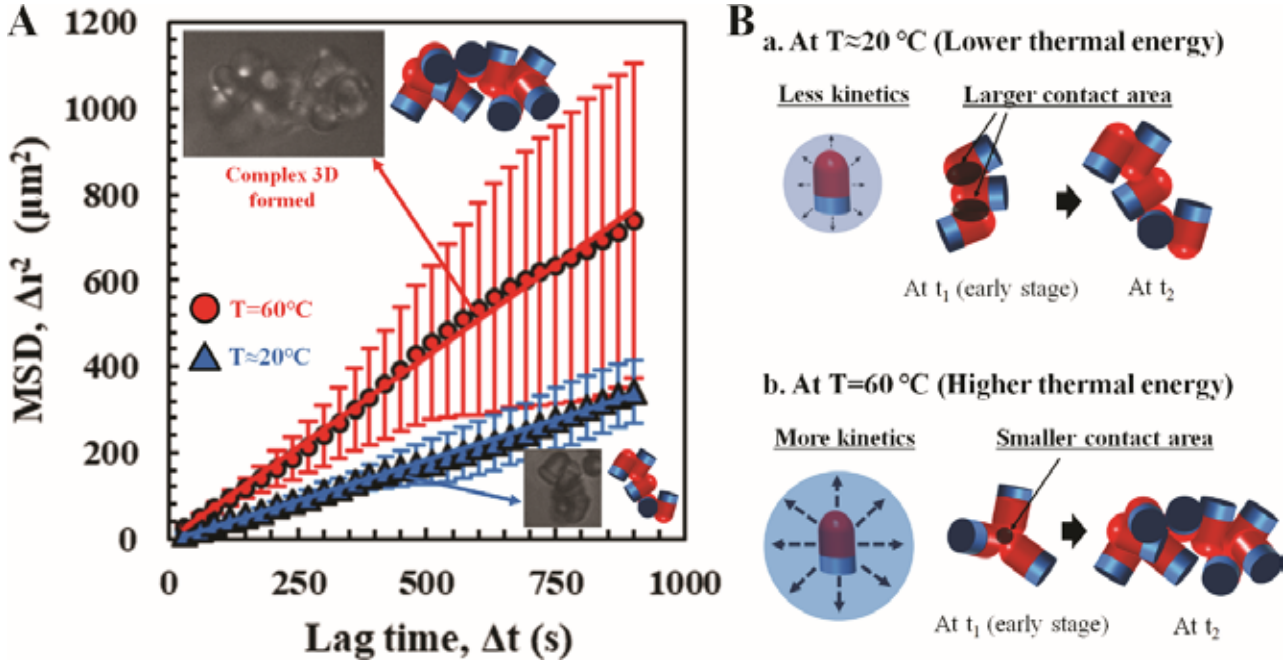

Figure 5. Temperature-dependent particle kinetics and their self-assembly. (A) The MSD of the Janus particles at each temperature (T≈20°C and T=60°C). A slope (red or blue) of the solid line divided by 4 yields the 2D translational diffusion coefficient of the 7:3 convex-top Janus particle at each temperature. The inset images show distinct 3D structures formed via self-assembly at each temperature: complex 3D clusters with smaller contact areas at 60°C and less complex 3D clusters with larger contact areas at 20°C. (B) Suggested behavior, interaction of the Janus particles, and 3D complex cluster formation at each temperature.

Table 2. 2D Translational diffusion coefficient (D_t) and collision frequency of the 7:3 convex-top Janus particle.

Conditions	Temperature		Thermal energy (k_BT)	Viscosity (η)	Translational diffusion coefficient (D_t)	Collision frequency (J)
	℃	K	N·μm	cP	μm²/s	sec⁻¹
Gravity	23.5	296.65	4.097×10^{-15}	0.899	3.773×10^{-2}	0.054
Microgravity	≈20	≈293.15	4.048×10^{-15}	1.002	9.378×10^{-2}	0.133
	60	333.15	4.601×10^{-15}	0.466	21.415×10^{-2}	0.304

The quantitative analysis in **Table 2** provides the 2D translational diffusion coefficient, indicating particles' mobility and the theoretically estimated kinetics of interparticle interaction at each temperature. First, the translational diffusion coefficient (D_t) of the 7:3 hydrophobic-to-hydrophilic ratio of the Janus particles at 60°C is 2.28 times greater than at 20°C, evidently showing that the Janus particles' random motion is quite active at higher temperatures. Next, the collision frequency between the Janus particles at two different temperatures (≈20°C and 60°C) is approximately assessed by employing the Smoluchowski equation (9) (Gregory, 2005; Wang et al., 2012) for estimation of the increased kinetics of the Janus particles.

$$J \approx 4\pi(r_i + r_j)(D_i + D_j)N_iN_j \quad (9)$$

Here, r is radius of the particles i and j (here we assumed the Janus particles as spheres for approximation), D is the translational diffusion coefficient of the particles i and j, and N is number of particles i and j per unit volume, respectively. Basically, the 7:3 convex-top Janus particles in microgravity collide 2.5 times more frequently (0.133 sec⁻¹) than under gravity (0.054 sec⁻¹). At a higher temperature (=60℃), the collision frequency further increases to 2.3 times (0.304 sec⁻¹). Notably, collisions occur every 3.289 seconds at 60℃, while the collision time extends to 7.518 seconds at lower temperature (≈20℃). The elevated collision frequency at a higher temperature enhances interaction kinetics, leading to the formation of larger and more complex 3D clusters, whereas smaller clusters emerge at a lower temperature. This temperature-mediated modulation of particle dynamics and assembly complexity is of considerable interest. It suggests

a methodology for controlling the self-assembly process of colloidal particles by adjusting the ambient temperature, thereby designing the final structures' complexity. The findings prove that by harnessing the thermodynamic parameters, it may be possible to engineer novel materials with customized properties, utilizing the unique conditions of microgravity and controlled temperature to steer the self-assembly processes of colloidal systems.

NASA's GRC, with its extensive experience and professional expertise in remote operations, has been integral to our mission operation. Their proficiency in remote control and data transfer processes has enabled the seamless operation of experimental parameter controls and data acquisition. The significant findings from our mission, such as Janus particles' movement, orientation, kinetics, and self-assembly in space without the masking effect of gravity, have enhanced our understanding of the fundamental behavior of anisotropic particles. It is promising to enrich colloidal and advanced materials science research with novel applications and functionalities in an extraterrestrial environment.

Discussion

By utilizing fascinating microgravity conditions, we demonstrate that chemically and geometrically well-controlled Janus particles are able to self-assemble into diverse 3D structures, encompassing spherical-like, densely packed, and linearly grown clusters via active Brownian motion. In contrast to gravitational conditions that result in hindering particle behavior, enforcing reorientation on a 2D planar plane and limiting growth kinetics, microgravity distinctly exposes the fundamental kinetics of particles and the formation of novel 3D structures at thermodynamic equilibrium. Another notable key finding is the significant impact of combinatorial anisotropy in the self-assembly of particles. This effect originates from the precisely controlled dual chemical properties, which incorporate opposing hydrophobic and hydrophilic groups, and finely manipulated geometric aspects such as the ratios of hydrophobic and hydrophilic parts as the majority, with the convex-top serving as an auxiliary feature. These factors collectively play a crucial role in determining the growth behavior and structural arrangement of the self-assembled particles.

A potential future study and enhancement involves closely observing the self-assembly behavior at an early stage with short intervals, providing in-depth understanding of growth kinetics and thermodynamic reorientation during continuous interparticle interaction. Regarding particle design, controlling the geometry of the top on hydrophobic parts is a potential approach for altering the configuration of interaction. The convex-top used in this study shows the uniform interaction area throughout the curved geometry, allowing interaction with a small contact area (tip-to-tip). Alternatively, designing a variety of polyhedral with a controlled number of faces and their angles holds the potential to stepwise control the degree of freedom for directionality. Additionally, triblock particles with hydrophobic parts at both ends have the potential to form consecutively and linearly grown structures, simulating propagation in polymer kinetics. These geometrically manipulated aspects are promising for controlling kinetics in growth as well as complexity in forms of self-assembly. From a chemical perspective, the incorporation of both negatively and positively charged hydrophilic parts on Janus particles can further balance or enhance interaction forces, including hydrophobic and additional ionic interactions, which potentially contributes to the complexity of self-assembly behavior.

Conclusions

In this study, we explore the self-assembly of anisotropic Janus particles under microgravity conditions, uncovering novel insights into the fundamental principles that govern particle assembly. The absence of gravity in our experiments allows for an observation of particle interactions and assembly dynamics, elucidating the intrinsic properties of anisotropic particles and their capacity to form complex structures.

Our investigation represents a substantial advancement in the fields of colloidal science and microgravity research, offering both theoretical insights and practical applications. The direct examination of anisotropic Janus particles' behavior within the microgravity conditions provided by the ISS enhances our understanding of colloidal dynamics free from gravitational influences. This study elucidates some underlying principles of self-assembly under microgravity conditions, demonstrating the capacity for the formation of 3D self-assembled clusters independent of sedimentation effects. These observations are crucial for the innovation of novel materials and the refinement of manufacturing processes that exploit these inherent phenomena.

Furthermore, this work will be extended to the design of next-generation materials with potential applications in various industries, such as pharmaceuticals, electronics, and space exploration. The ability to form new structures in microgravity could lead to the synthesis of new materials with novel properties, such as improved catalysts, targeted drug delivery systems, and advanced optical devices.

Finally, this research emphasizes the importance of international collaboration in space exploration and science. By collaborating with NASA's GRC and utilizing the ISS's facilities, this study confirms the collaborative efforts required to push the boundaries of what is possible in materials science and space research. We envision this study serving

as a cornerstone for further research into the design and synthesis of innovative materials in microgravity. The insights gained here not only advance our understanding of particle assembly but also underscore the transformative potential of collaborative space research.

Acknowledgments

This work was supported by the National Research Foundation of Korea (NRF) grant funded by the Korean government (MSIT) (No. 2021R1A2C3004936 and 2021R1A5A8032895). Special thanks to the members of NASA's GRC, ZIN Technology, and KBR Wyle Services, particularly Amber Abbott for scheduling and planning; Beth Curtis for coordination with ISS planners at MSFC to coordinate FIR/ACET1 scheduling and serving as the rack officer (RO) and data management officer (DMO); Stetmond Roberson for coordination with the PI to develop the Daily Operations Plan (DOP) and serving as the RO and the DMO; Charles Bunnell, Louis Chestney, Emily Johnson, and Yinan Li for the development of payload and operation of the microscope within the FIR; Helen Brown, Sarah Czerwien, Sam Dunton, Emily Griffin, Amber Krauss, Andrea Marchica, Teresa Miller, and Jonathan Rodriguez-Lucas for serving as ROs and DMOs responsible for the FIR rack during powered ops.

Author Disclosure Statement

No competing financial interests exist.

References

Bailey AE, Poon WCK, Christianson RJ, Schofield AB, Gasser U, Prasad V, Manley S, Segre PN, Cipelletti L, Meyer WV, Doherty MP, Sankaran S, Jankovsky AL, Shiley WL, Bowen JP, Eggers JC, Kurta C, Lorik T, Pusey PN, Weitz DA (2007) Spinodal decomposition in a model colloid-polymer mixture in microgravity. *Physical Review Letters* **99**: 205701-1-205701-4

Baldwin RL (1986) Temperature-dependence of the hydrophobic interaction in protein folding. *Proceedings of the National Academy of Sciences of the United States of America* **83**: 8069-8072

Carrasco B, de la Torre JG (1999) Hydrodynamic properties of rigid particles: Comparison of different modeling and computational procedures. *Biophysical Journal* **76**: 3044-3057

Cheng ZD, Chaikin PM, Zhu JX, Russel WB, Meyer WV (2002) Crystallization kinetics of hard spheres in microgravity in the coexistence regime: Interactions between growing crystallites. *Physical Review Letters* **88**: 015501-1-015501-4

Choi CH, Lee J, Yoon K, Tripathi A, Stone HA, Weitz DA, Lee CS (2010) Surface-tension-induced synthesis of complex particles using confined polymeric fluids. *Angewandte Chemie-International Edition* **49**: 7748-7752

Claesson PM, Kjellander R, Stenius P, Christenson HK (1986) Direct measurement of temperature-dependent interactions between non-ionic surfactant layers. *Journal of the Chemical Society, Faraday Transactions 1: Physical Chemistry in Condensed Phases* **82**: 2735-2746

Delatorre JG, Bloomfield VA (1981) Hydrodynamic properties of complex, rigid, biological macromolecules - theory and applications. *Quarterly Reviews of Biophysics* **14**: 81-139

Dinsmore AD, Crocker JC, Yodh AG (1998) Self-assembly of colloidal crystals. *Current Opinion in Colloid & Interface Science* **3**: 5-11

Glotzer SC, Solomon MJ (2007) Anisotropy of building blocks and their assembly into complex structures. *Nature Materials* **6**: 557-562

Gregory J (2005) *Particles in Water: Properties and Processes*, Boca Raton: CRC Press.

Grzybowski BA, Winkleman A, Wiles JA, Brumer Y, Whitesides GM (2003) Electrostatic self-assembly of macroscopic crystals using contact electrification. *Nature Materials* **2**: 241-245

Kegel WK, van der Schoot P (2004) Competing hydrophobic and screened-Coulomb interactions in hepatitis B virus capsid assembly. *Biophysical Journal* **86**: 3905-3913

Lee MH, Furst EM (2006) Formation and evolution of sediment layers in an aggregating colloidal suspension. *Physical Review E* **74**: 031401-1-031401-11

Lin KH, Crocker JC, Prasad V, Schofield A, Weitz DA, Lubensky TC, Yodh AG (2000) Entropically driven colloidal crystallization on patterned surfaces. *Physical Review Letters* **85**: 1770-1773

Manley S, Cipelletti L, Trappe V, Bailey AE, Christianson RJ, Gasser U, Prasad V, Segre PN, Doherty MP, Sankaran S, Jankovsky AL, Shiley B, Bowen J, Eggers J, Kurta C, Lorik T, Weitz DA (2004) Limits to gelation in colloidal aggregation. *Physical Review Letters* **93**: 108302-1-108302-4

Napper DH (1983) *Polymeric Stabilization of Colloidal Dispersions*, London, New York: Academic Press.

Némethy G, Scheraga HA (1962) The structure of water and hydrophobic bonding in proteins. iii. The thermodynamic properties of hydrophobic bonds in proteins1, 2. *The Journal of Physical Chemistry* **66**: 1773-1789

Ortega A, de la Torre JG (2003) Hydrodynamic properties of rodlike and disklike particles in dilute solution. *Journal of Chemical Physics* **119**: 9914-9919

Oss CJv (2006) *Interfacial Forces in Aqueous Media*, Boca Raton: CRC Press.

Sedgwick H, Egelhaaf SU, Poon WCK (2004) Clusters and gels in systems of sticky particles. *Journal of Physics-Condensed Matter* **16**: S4913-S4922

Segrè PN, Prasad V, Schofield AB, Weitz DA (2001) Glasslike kinetic arrest at the colloidal-gelation transition. *Physical Review Letters* **86**: 6042-6045

Senis D, Allain C (1997) Scaling analysis of sediment equilibrium in aggregated colloidal suspensions. *Physical Review E* **55**: 7797-7800

Tadros TF (2015) *Interfacial Phenomena and Colloid Stability*, Berlin, München, Boston: De Gruyter.

Tirado MM, Martinez CL, Delatorre JG (1984) Comparison of theories for the translational and rotational diffusion-coefficients of rod-like macromolecules - application to short DNA fragments. *Journal of Chemical Physics* **81**: 2047-2052

Vanoss CJ, Chaudhury MK, Good RJ (1988) Interfacial lifshitz-vanderwaals and polar interactions in macroscopic systems. *Chemical Reviews* **88**: 927-941

Wang YF, Wang Y, Breed DR, Manoharan VN, Feng L, Hollingsworth AD, Weck M, Pine DJ (2012) Colloids with valence and specific directional bonding. *Nature* **491**: 51-U61

Weeks JR, van Duijneveldt JS, Vincent B (2000) Formation and collapse of gels of sterically stabilized colloidal particles. *Journal of Physics-Condensed Matter* **12**: 9599-9606

Whitmer JK, Luijten E (2011) Sedimentation of aggregating colloids. *Journal of Chemical Physics* **134**: 034510-1-034510-10

Yeom SJ, Kang SM, Kim J, Nam JO, Eom N, Lee S, Lee CS (2016) Fabrication of multicompartment particles via sequential micromolding method. *Polymer-Korea* **40**: 457-463

Zhu JX, Li M, Rogers R, Meyer W, Ottewill RH, Russell WB, Chaikin PM (1997) Crystallization of hard-sphere colloids in microgravity. *Nature* **387**: 883-885